

OwlSight: A Robust Illumination Adaptation Framework for Dark Video Human Action Recognition

Shihao Cheng^{*1} Jinlu Zhang^{*2} Yue Liu¹ Zhigang Tu^{1†}
¹Wuhan University ²Peking University

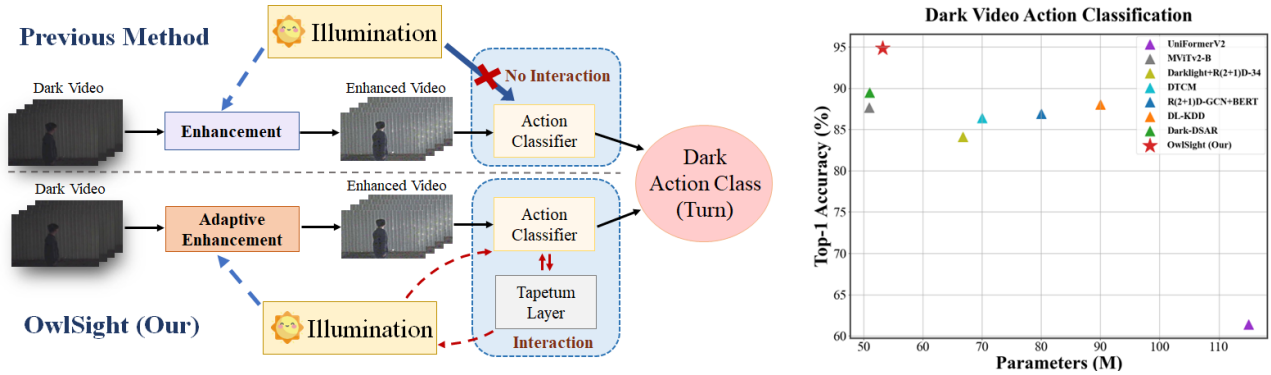


Figure 1. **Left:** Overview of our OwlSight. In contrast to the previous methods, we place a strong emphasis on fully exploring and utilizing illumination information throughout all stages interactively to boost the performance of dark video action recognition. **Right:** Accuracy (Top-1 Accuracy) and efficiency (parameters) comparison with the state-of-the-arts on the ARID1.5 [39] dataset.

Abstract

Human action recognition in low-light environments is crucial for various real-world applications. However, the existing approaches overlook the full utilization of brightness information throughout the training phase, leading to suboptimal performance. To address this limitation, we propose OwlSight, a biomimetic-inspired framework with whole-stage illumination enhancement to interact with action classification for accurate dark video human action recognition. Specifically, OwlSight incorporates a Time-Consistency Module (TCM) to capture shallow spatiotemporal features meanwhile maintaining temporal coherence, which are then processed by a Luminance Adaptation Module (LAM) to dynamically adjust the brightness based on the input luminance distribution. Furthermore, a Reflect Augmentation Module (RAM) is presented to maximize illumination utilization and simultaneously enhance action recognition via two interactive paths. Additionally, we build **Dark-101**, a large-scale dataset comprising 18,310 dark videos across 101 action categories, significantly surpassing existing datasets (e.g., ARID1.5 and Dark-48) in scale and diversity. Extensive experiments demonstrate that the proposed OwlSight achieves the state-of-the-art per-

formance across four low-light action recognition benchmarks. Notably, it outperforms prior best approaches by **5.36% on ARID1.5** and **1.72% on our Dark-101**, highlighting its effectiveness in challenging dark environments.

1. Introduction

Recognizing human actions in dark videos is a useful yet challenging visual task in real-world scenarios. It aims to identify human actions in conditions of low brightness and low contrast, which can benefit a large range of applications, such as video security surveillance, vision-based autonomous driving systems, etc.

Given its practical significance, numerous methods have been proposed for action recognition in low-light videos. However, these methods have certain limitations. Some studies seek to enhance action recognition in low-quality videos by integrating sensor data beyond RGB video. For example, [44] uses infrared data features to improve action recognition accuracy in dark environments. However, the incorporation of additional sensor data significantly increases costs, complicates deployment configura-

^{*}Shihao Cheng and Jinlu Zhang contributed equally to this work.

[†]Zhigang Tu is the corresponding author (tuzhigang@whu.edu.cn).

tions, and adds to processing complexity. On the other hand, augmentation-based methods [9] are also widely used, where they typically apply Low-Light Video Enhancement (LLVE) to boost the visual quality of low-illumination videos before utilizing the enhanced video frames for action recognition. However, LLVE methods often depend on optical flow, coming with high computational cost. Alarming, the prior research [39] has shown that most illumination enhancement techniques do not improve action recognition performance in dark videos, as their task coherence tends to be fragmented.

Recently, one-stage low-light video action recognition methods have been presented [34], allowing the entire network to be trained in a single phase. However, these methods primarily focus on illumination enhancement as a pre-processing step, rather than integrating illumination adaptation directly into the training process, which limits their effectiveness in enhancing recognition performance.

Studying night vision in biological systems [14] reveals that creatures with enhanced night vision possess unique visual adaptations. As illustrated in Figure 2, in dim light, the pupil adjusts its size based on brightness, regulating light entry. Unabsorbed light is then reflected by the tapetum, a layer behind the retina, providing a second opportunity for light capture and improving visual clarity.

Drawing inspiration from this biological mechanism, we propose OwlSight, an end-to-end trained model designed for action recognition in low-light environments, as shown in Figure 1. Firstly, the lightweight Time-Consistency Module (TCM) is designed to capture shallow spatiotemporal features. Secondly, these features are processed by an exploited Luminance Adaptation Module (LAM), which adaptively adjusts global brightness based on the input illumination distribution. Thirdly, the adjusted features are passed to a Reflect Augmentation Module (RAM), which processes the input features to generate a ‘reflected’ version, subsequently handled via a specialized encoder. By integrating the reflected features with the input features across multiple stages, RAM maximizes the usage of the available illumination information.

Noticeably, as models scale up, existing datasets like ARID [39] and ARID1.5 [39] are constrained in small-scale. Dark-48 [34] contains many redundant videos and lacks action-specific content. Synthetic datasets like UAVHuman-Night [16] do not capture the natural vision and uneven lighting that are presented in real low-light environments. To address these issues, we constructed a new large-scale dataset called Dark-101, which is composed of 15,621 low-light videos spanning 101 action categories in 138 diverse scenes.

Our key contributions are summarized as follows:

- We propose **OwlSight**, a biomimetic-inspired framework to fully exploit illumination information for dark action

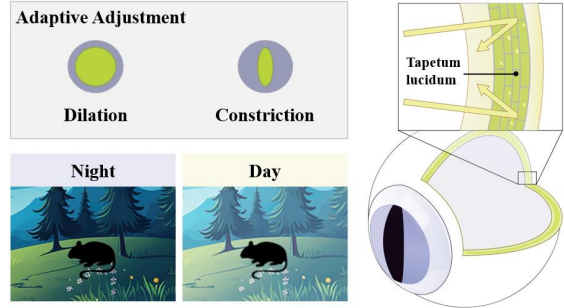


Figure 2. **Left:** Nocturnal animals dilate pupils at night for capturing enhanced light and constrict them during the day to avoid overexposure. **Right:** The tapetum lucidum, a reflective retinal layer, reflects light to improve illumination and visual clarity.

recognition in the whole training stage interactively.

- We introduce a **Luminance Adaptation Module (LAM)** and a **Reflect Augmentation Module (RAM)**, where LAM adaptively adjusts the global brightness based on the input illumination distribution, RAM generates a reflected version of the input features and merges them with the original features to leverage illumination interactively.
- We present **Dark-101**, a large-scale low-light video dataset composed of 18,310 samples across 101 action categories, more than 2 times bigger than the previous ones (18310 vs. 8815), enabling to train larger dark video action recognition models.
- Extensive experiments demonstrate that our OwlSight achieves the state-of-the-art performance across four low-light action recognition benchmark datasets, e.g. it surpasses the previous methods by **5.36%** on the widely-used dataset ARID1.5 [39].

2. Related Work

2.1. Low-light Image and Video Enhancement

Existing image enhancement methods can be divided into traditional methods and deep learning-based methods. Traditional methods include histogram equalization, gamma correction, and dark light enhancement techniques based on the Retinex theory. Deep learning-based methods can be classified into several categories: 1) Zero-shot learning-based methods, which do not rely on paired training data, such as Zero-DCE [11] and RRDNet [43]. Zero-DCE [11] transforms the low-light enhancement problem into an image-specific curve estimation problem, achieving image enhancement via a non-reference loss function. 2) Reinforcement learning-based methods, which utilize deep reinforcement learning for exposure optimization. For example, DeepExposure [42] automatically learns local exposure for each sub-image meanwhile globally designs rewards to balance overall exposure. 3) Unsupervised learning-

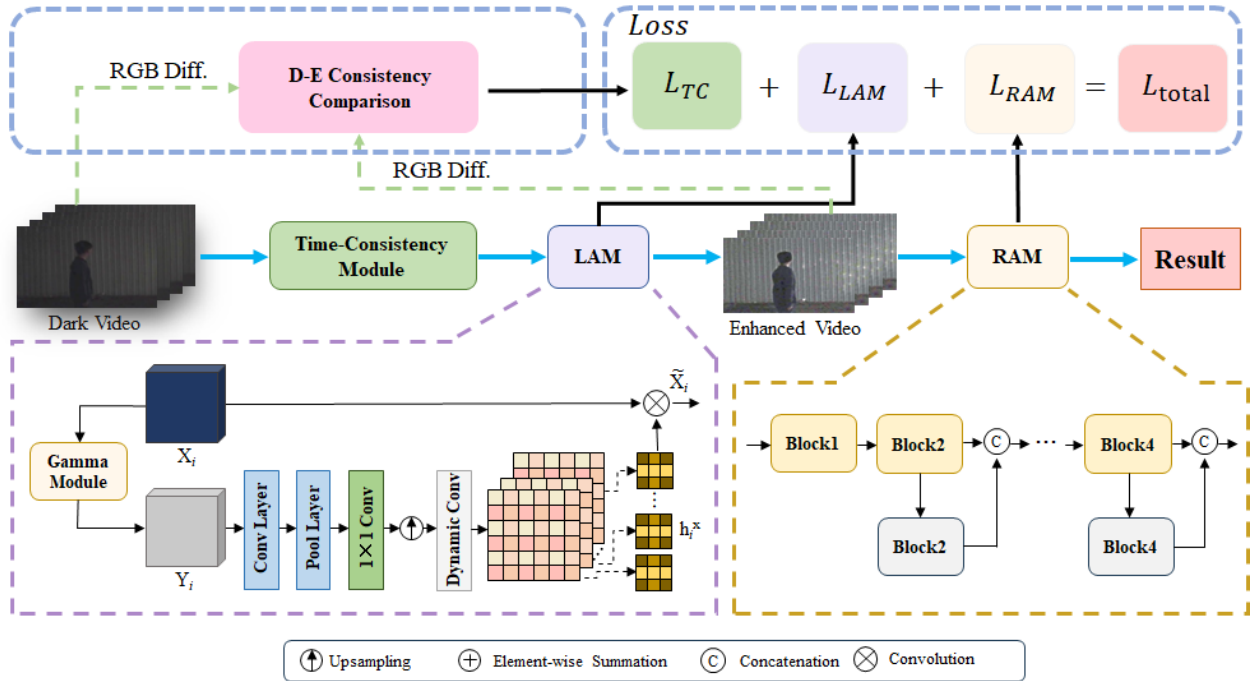


Figure 3. **The Overall Architecture of OwlSight.** OwlSight consists of three key components: the Time-Consistency Module (TCM), the Luminance Adaptation Module (LAM), and the Reflect Augmentation Module (RAM). The TCM extracts shallow spatiotemporal features to preserve temporal coherence across the sequence. The LAM adaptively adjusts global brightness based on the input luminance distribution. The RAM further enhances available illumination meanwhile improving action recognition through two interactive pathways. The Dark-Enhanced (D-E) consistency of the video frames, which is beneficial for video action recognition in low-light environments, can be preserved by comparing the RGB-difference before and after dark video enhancement.

based methods, which also do not require paired training data. E.g., EnlightenGAN [13] enhances low-light images using GANs, and PairLIE [8] uses paired weak-light instances for training. 4) Supervised learning-based methods, which require a large amount of labeled data for training, like [2, 19, 23, 33, 37, 38, 40, 44]. CIDNet [40] introduces HVI color space and enhances images through a dual-path approach. Retinexformer [2] combines Retinex theory with transformers. However, directly applying low-light enhancement to videos can lead to temporal consistency issues, which is why LLVE was proposed. MBLLVEN [24] extracts temporal information using 3D convolutions to maintain temporal consistency. StableLLVE [17] maintains temporal consistency in enhanced videos by learning and inferring motion fields (i.e. optical flow) from synthesized short-distance video sequences. Our method also considers the correlation and consistency across temporal dimension, where we present a lightweight slow-fast time consistency module to effectively ensure temporal smoothness in video.

2.2. Dark video Action Recognition

Initially, conventional action recognition methods, such as C3D [31], P3D ResNet [26], and I3D [3], were introduced to tackle visual tasks under low-light conditions. However, these methods are not well-suited for challenging dark environments. Existing approaches for action recognition in dark videos can be broadly categorized into three types: modality-assisted methods, two-stage augmentation methods, and one-stage augmentation methods.

Modality-assisted methods boost action recognition in low-quality video with the help of some sensor information other than RGB video. Ulhaq [35] fused multiple video stream deep features corresponding to multiple spectra to combine visible light sequences with infrared data features in night vision scenes. For augmentation-based two-stage methods, DarkLight [6] enhances videos using gamma correction and applies action recognition through a dual-path approach. The two-stream action recognition method [30] builds on this dual-path framework, using self-calibrated supervision (SCI) [32] with temporal graph encoding for action recognition. For augment-based one-stage methods,

DTCM [34] achieves end-to-end learning and introduces a dedicated dark video dataset, Dark48. DSAR [41] extends this structure by integrating MViTv2 [18] with dark enhancement techniques, yielding further improvements.

To achieve more efficient and accurate action recognition, our model, OwlSight, integrates a nocturnal vision mechanism with a Transformer-based architecture, enabling flexible capture of multi-scale spatiotemporal features in low-light scenes, and interactively utilizing illumination information through dual pathways.

2.3. Low-Light Action Recognition Datasets

Low-light video action recognition has been advanced by several key datasets. ARID [39] is one of the earliest datasets, containing 3,784 video clips across 11 action categories, all captured in dark environments. However, its limited size restricts model training. To address this, ARID1.5 [39] expands the dataset by adding more action categories and varying lighting conditions, resulting in a total of 5,572 video clips. Nonetheless, the dataset remains relatively small, and the individual video durations are brief. Subsequently, Dark-48 [34] offers a larger and more diverse collection, with 48 action categories and 8,815 video clips, enhancing testing conditions for low-light scenarios. However, the limited number of categories still poses challenges for comprehensive model training. UAVHuman-Night [16] focuses on aerial videos captured by drones, including both daytime and nighttime sequences, which is particularly beneficial for low-light surveillance applications.

To address the limitations related to dataset size, category diversity, short video duration, etc., we design Dark-101, a high-quality dataset that includes 15,621 video clips across multiple scenes with longer video durations, enabling support more generalized and robust low-light action recognition investigation.

3. Proposed Method

As shown in Fig. 3, OwlSight is composed of three main components: the Temporal-Consistency Module, the Luminance Adaptation Module (LAM), and the Reflective Augmentation Module (RAM). Our method first employs the Temporal-Consistency Module to extract shallow spatiotemporal information. Then, LAM adaptively utilizes available illumination information, and RAM further enhances illumination through two interactive pathways, progressively benefiting recognition performance. The entire network is trained end-to-end, effectively integrating both enhancement and recognition.

3.1. Time-Consistency Module

The architecture of the Time-Consistency Module is illustrated in Fig. 4. For a low-light input video $\{F_i\}_{i=1}^T \in \mathbb{R}^{T \times 3 \times H \times W}$, where T denotes the number of video frames,

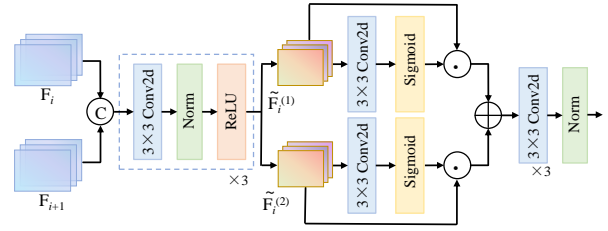


Figure 4. Architecture of the Time-Consistency Module.

we first concatenate adjacent frames F_i and F_{i+1} to obtain the paired sequence $\{(F_i, F_{i+1})\}$. This sequence is initially processed by a shallow convolutional network with a kernel size of 3×3 and a stride of 1, followed by a normalization layer and a ReLU activation function. This processing sequence is repeated three times to progressively extract shallow features \tilde{F}_i , which has a spatial dimension of $H \times W$ and a channel dimension of $2C$. Next, we split \tilde{F}_i into two separate components, $\tilde{F}_i^{(1)}$ and $\tilde{F}_i^{(2)}$, along the channel dimension on average. The Inter-frame features z are obtained as:

$$z = \tilde{F}_i^{(1)} \cdot \sigma(W_{3 \times 3}(\tilde{F}_i^{(1)})) + \tilde{F}_i^{(2)} \cdot \sigma(W_{3 \times 3}(\tilde{F}_i^{(2)})), \quad (1)$$

where $W_{3 \times 3}(\cdot)$ denotes the 3×3 convolution operation, and σ represents the sigmoid activation function. The outputs z are then passed through three 3×3 convolutional layers followed by normalization for subsequent feature mixing. The spatiotemporal features X_i are subsequently extracted and fed into the LAM for enhancement.

To preserve temporal coherence across the frame sequence, we adopt the meticulously crafted loss functions from DTCM [34], which are defined as follows:

$$L_{TC} = \frac{1}{T-1} \sum_{t=1}^{T-1} L_{SCF} (|DY_{t+1} - DY_t|, |DI_{t+1} - DI_t|), \quad (2)$$

where T is the number of input video clip duration, L_{SCF} measures the discrepancy between the temporal variations of the enhanced and input video frames. $|DY_{t+1} - DY_t|$ and $|DI_{t+1} - DI_t|$ represent the RGB-Difference of the enhanced frame and the dark frame, respectively. See the Supplemental Materials for more details.

3.2. Luminance Adaptation Module

We propose the Luminance Adaptation Module (LAM), inspired by the visual adaptation mechanisms observed in nocturnal animals. Many nocturnal species possess the ability to adaptively adjust the response of photoreceptor cells in their retinas, thereby enhancing visual acuity in low-light environments. Similarly, the LAM is designed to dynamically adjust pixel-wise filters in response to local luminance

variations in the input image, improving feature extraction under varying lighting conditions.

Specifically, the input feature map X_i first undergoes a Gamma Module to adjust its luminance mean. This adjustment is achieved by calculating the luminance mean μ_{in} of the input image and applying a Gamma transformation to scale the image’s luminance. The Gamma value γ is computed using the following formula:

$$\gamma = \frac{\log(\mu_{\text{out}})}{\log(\mu_{\text{in}})}, \quad (3)$$

where μ_{out} is the target luminance mean and μ_{in} is the luminance mean of the input image. Based on the experiments, we set $\mu_{\text{out}} = 0.5$. The details of the experiments can be found in Section 4.3. We initially normalize the input features X_i to the range $[0, 1]$ to obtain X'_i . Subsequently, the formula for conducting the illumination transformation on the normalized input features X'_i is presented as follows:

$$Y_i = X'_i{}^\gamma. \quad (4)$$

The adjusted image is passed through a series of downsampling and feature extraction layers, including average pooling, max pooling, and two residual blocks, capturing multi-scale luminance information.

Next, a 1×1 convolutional layer generates filter weights that are adaptively adjusted based on the luminance information at each pixel. These pixel-wise filters, denoted h_i^x , are then convolved with local image patches $R(X_i)$ to produce the adaptive output features:

$$\hat{X}_i(x) = h_i^x \otimes R(X_i), \quad (5)$$

where h_i^x is a filter with size $u_p \times u_p$, ensuring each pixel position generates an adaptive filtering effect based on the surrounding luminance. This adaptive design enhances the model’s ability to handle complex lighting variations, facilitating more robust image information extraction.

The overall and pixel-by-pixel illumination adjustments should be jointly considered during training, as both global illumination enhancement and preservation of the original semantics during the brightness enhancement process are necessary. We use the loss functions that are well designed by Zero-IG [28] expressed as:

$$L_{\text{LAM}} = L_{\text{over}} + L_{\text{pix}}, \quad (6)$$

L_{over} represents the overall adjustment loss, L_{pix} denotes the pixel-by-pixel adjustment loss. In this study, we adopt the same settings for the loss functions as those used in Zero-IG [28]. See the Supplemental Materials for more details.

3.3. Reflect Augmentation Module

In low-light action recognition, effectively capturing and utilizing illumination is crucial. Previous approaches typ-

ically handle illumination enhancement and action recognition separately, leading to suboptimal usage of available light. To address this, we introduce the Reflect Augmentation Module (RAM), featuring a dual-channel interactive illumination compensator designed to fully exploit ambient illumination directly within the recognition framework.

In RAM, each input feature X_i undergoes deep processing through a dual-pathway structure. First, X_i is passed through the action recognition backbone of DSAR, which serves as the main pathway and is denoted by $f_1(X_i)$. The output features from the main pathway are then passed to the reflected pathway, which has the same structure as the main pathway, but each stage retains only a single transformer block for lightweight processing. In the reflected pathway, the “reflected features” capture latent global illumination dynamics, which are crucial for feature representation in low-light scenarios. The features from both the reflected and main pathways are then fused via combination \odot . This process not only fuses the features but also preserves spatially unique information from both two pathways. The entire process is defined as follows:

$$X_{i+1} = f_2(f_1(X_i)) \odot f_1(X_i), \quad (7)$$

where f_1 represents the core computation for the main pathway, f_2 denotes the reflected pathway, and \odot represents the concatenation operation.

This architecture enables RAM to adaptively accumulate illumination-sensitive features across stages, facilitating robust action recognition under challenging low-light conditions. Each stage output X_{i+1} incorporates multi-scale illumination corrections, significantly enhancing the model’s performance in dark environments.

The loss function for RAM is the standard cross-entropy loss, where y denotes the action category and \hat{y} is the predicted category, which is defined as:

$$L_{\text{RAM}} = - \sum_i y_i \log(\hat{y}_i). \quad (8)$$

Since our method is trained end-to-end, the total loss function is defined as: $L_{\text{total}} = L_{\text{TC}} + L_{\text{LAM}} + L_{\text{RAM}}$.

3.4. Dark-101

As we have described in the Introduction section that the existing low-light action recognition datasets have some limitations. ARID [39] contains only 3,784 videos and ARID1.5 [39] expands to 5,572 videos, but both remain relatively small, with limited action categories and scenes. Recently, Dark-48 [34] enlarged the scale to 8,815 videos across 48 categories but included amounts of noise videos unrelated to actions, resulting in suboptimal training outcomes.

To address these challenges and meet the demand of training deep learning big models, constructing a large-scale dataset is extremely urgent. However, building a completely new dark video dataset with a much larger number of videos and action categories is difficult. We collect useful dark videos from existing benchmarks economically and the Internet painstakingly.

Dataset	Actions	Scenes	Total
ARID [39]	11	18	3784
ARID1.5 [39]	11	24	5572
Dark-48 [34]	48	52	8815
Dark-101	101	138	18310

Table 1. Comparison of Dark Video Action Recognition Datasets: ARID [39], ARID1.5 [39], Dark-48 [34], and our Dark-101. ‘Actions’ indicates the number of action classes, with each class comprising over 100 dark videos; ‘Scenes’ represents the number of distinct scenes from which the videos are sourced; ‘Total’ denotes the overall count of video clips.

Specifically, to get valuable data from the existing dataset, we first defined an evaluation metric called Global Darkness Quantification (GDQ). It combines the mean brightness of video frames with intra-frame brightness fluctuation to produce a quantified darkness index, distinguishing low-light videos from the normal-light ones.

For each video frame $I_t(x, y)$, (x, y) are pixel coordinates, the mean brightness μ_t is calculated as:

$$\mu_t = \frac{1}{M \cdot N} \sum_{x=1}^M \sum_{y=1}^N I_t(x, y), \quad (9)$$

where M and N represent the frame’s height and width.

To obtain a global brightness baseline, we calculate the average brightness μ_c across all video frames T :

$$\mu_c = \frac{1}{T} \sum_{t=1}^T \mu_t. \quad (10)$$

The darkness index D_v quantifies a video’s darkness by combining the difference between each frame’s brightness μ_t and the global average μ_c with the intra-frame brightness fluctuation σ_t (the standard deviation), which is defined as:

$$D_v = \frac{1}{T} \sum_{t=1}^T \left(\frac{\mu_t - \mu_c}{\sigma_t} \right) \cdot \sigma_t. \quad (11)$$

The video is classified as low-light if $D_v < -\tau$, otherwise as normal-light. Where τ is determined by the average darkness across all videos in ARID1.5 as [34] ($\tau = 0.877$).

To align with the darkness of the ARID1.5 dataset, we first evaluate the darkness of each video via our designed

video darkness evaluation measure Eq. 11. Moreover, we crawl a substantial amount of video data from the Internet publicly. The sources encompass platforms like YouTube. Specifically, among all the data we collected, 2689 videos are captured from the Internet and 15621 videos are selected from existing datasets, including Kinetics700 [4], Dark-48 [34], Something-Something V3 [10] and MIT [25]. We count the categories of the selected dark videos and retain only those categories with more than 150 videos, helping to solve the problem of long-tail distributions.

Compared with the previous datasets, our dataset exhibits a significantly lower illumination levels, a substantially larger number of videos, a more extensive variety of action categories, and a greater diversity of video scenarios. Besides, the duration of the videos ranges from 5 to 10 seconds, which is longer than that of the previous datasets (approximately 3 seconds). Consequently, it is possible to train models that with more powerful temporal extraction capability, and larger-size models that are not only more robust but also more generalized in application. The training and testing sets are partitioned by assigning 80% of the videos to the training set and the remaining 20% to the testing set. A statistical comparison among Dark-101, ARID, ARID1.5 [39], and Dark-48 [34] is given in Table 1. More details can be seen in the Supplemental Materials.

4. Experiment Results

4.1. Implementation Details

Parameter Settings. All experiments are implemented with PyTorch on 8 Nvidia 4090 GPUs. The ADAM optimizer is employed, with parameters $\beta_1 = 0.9$, $\beta_2 = 0.999$, and $\epsilon = 10^{-8}$. The batch size is set to 8 and learning rate is fixed at 2×10^{-4} . The training epoch number is set to 100.

Compared Methods. We compare our method OwlSight with several state-of-the-art low-light action recognition methods, e.g. Dark-DSAR [41], DTCM [34], DL-KDD [5], R(2+1)D-GCN+BERT [29], Darklight+R(2+1)D-34 [6]. The results are reproduced using the publicly available source codes with the recommended parameters.

Benchmarks Description and Metrics. We conduct experiments on four representative dark video action recognition datasets: ARID [39], ARID1.5 [39], Dark-48 [34], and our Dark-101. We evaluate the performance via Top-1 and Top-5 accuracy. For ARID1.5, both Top-1 and Top-5 are reported due to its being the most widely used dark video dataset. For other datasets, we report only Top-1 accuracy. Dark action recognition results for relevant methods are taken from their original papers, while for those without available results, we reproduce them (marked with *).

Model	Pretrained	Top-1 (%)	Top-5 (%)
TSN [36]	K400	34.04	88.29
TSM [20]	K400	61.37	91.80
SlowFast [7]	K400	66.76	91.58
R(2+1)D [32]	K400	63.52	92.29
Swin-T [22]	K400	67.69	97.55
TimeSformer [1]	K400	49.36	93.17
UniFormerV2 [15]	K400	61.41	96.04
MViTv2-B [18]	K400	87.68	98.55
Darklight+R(2+1)D-34 [6]	IG65M	84.13	97.34
DTCM* [34]	K400	86.42	97.28
R(2+1)D-GCN+BERT [29]	IG65M	86.93	99.35
Dark-DSAR [41]	K400	89.49	98.77
OwlSight	K400	94.85	99.50

Table 2. Comparison with the state-of-the-arts on the ARID1.5 [39] dataset. All results are calculated using the RGB channel. Red and blue colors indicate the best and second-best performance, respectively. The superscript * indicates the model is retrained on ARID1.5.

4.2. Benchmark Evaluations

Performance Evaluation. Our method OwlSight is evaluated with 32-frame inputs, sampled at 3-frame intervals, using standard data augmentation techniques like random resized cropping, horizontal flipping, and random erasing. In quantitative comparisons, our method outperforms others on ARID1.5 and ARID datasets, as presented in Table 2 and 3. Furthermore, on both Dark-48 and Dark-101 datasets, our method demonstrates superior performance over other existing algorithms. Due to space limitation, more comparisons are available in the Supplemental Materials.

Model	Top-1 (%)
Pseudo-3D-199 [26]	71.93
UniFormerV2 [15]	73.39
TimeSformer-L [1]	81.39
Video-Swin-B [22]	89.79
MViTv2-B [18]	91.43
DarkLight-R(2+1)D-34 [6]	94.34
Suman [30] et al.	95.86
Dark-DSAR [41]	96.99
DL-KDD [5]	97.27
OwlSight	99.27

Table 3. Comparison with state-of-the-arts on ARID.

4.3. Ablation Study

To evaluate the impact and performance of each component in our OwlSight, we examine their function in this section. For testing, we select the representative dataset ARID1.5.

Effect of Each Component. As shown in Table 4, the Baseline model is obtained by removing the LAM, RAM (only the reflected pathway) and TCM from our OwlSight, without applying any additional optimizations. The function of the LAM is to adaptively adjust the input low-light

video to normal illumination based on the input brightness range. When the LAM is removed, accuracy decreases by 2.45%, from 94.85% to 92.4%. Which demonstrates the adaptive illumination enhancement of LAM is effective. When the RAM is removed, accuracy drops by 3.03%, from 94.85% to 91.82%. This is because the designed RAM aims to interactively exploit illumination information for better recognition. Without it, OwlSight loses one pathway for leveraging the illumination information. When the TCM is removed, the results show a 1.81% reduction in accuracy, from 94.85% to 93.04%. Which reveals preserving temporal coherence across the enhanced frame sequence is helpful for dark video recognition.

	LAM	RAM	TCM	Top-1 (%)
Baseline	✗	✗	✗	87.68
	✗	✓	✓	92.40
	✓	✗	✓	91.82
	✓	✓	✗	93.04
OwlSight	✓	✓	✓	94.85

Table 4. Ablation study of each component in our model OwlSight. The Top-1 Accuracy on ARID1.5 is reported.

L_{ar}	L_{TC}	L_{over}	L_{pix}	Top-1 (%)
✓	✗	✓	✓	92.03
✓	✓	✗	✓	91.32
✓	✓	✓	✗	91.25
✓	✓	✓	✓	94.85

Table 5. Ablation study of the loss terms in our OwlSight.

Effect of Loss Function. We explore the contribution of our loss function in detail. Since the cross-entropy L_{ar} used by L_{RAM} determines the final classification result, it cannot be removed. As shown in Table 5, the Top-1 accu-

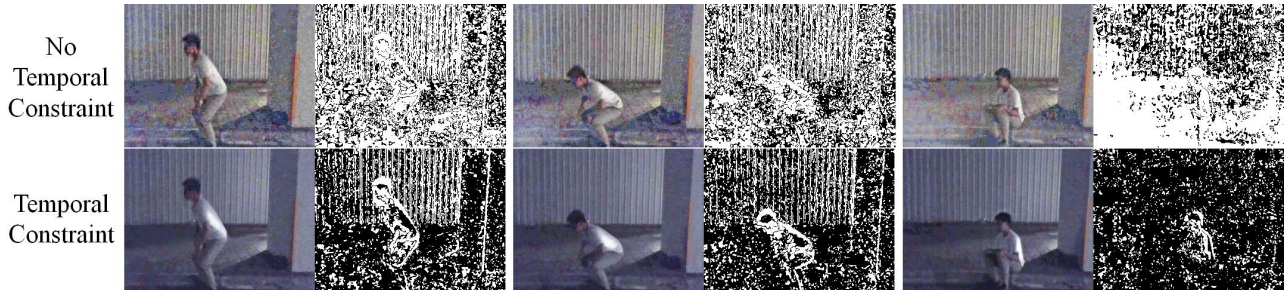


Figure 5. Comparison of RGB-Difference of our OwlSight with and without temporal constraint (TCM and L_{TC}) on the ARID1.5 dataset. Results are as follows: The upper part shows the RGB-Difference of OwlSight without temporal constraint, which are failed to improve the action recognition performance in dark videos. The lower part shows the RGB-Difference of OwlSight with temporal constrain. Obviously, the introduced temporal constraint strategy significantly boosts the performance of action recognition in dark videos.

racy decreases from 94.85% to 91.25% after removing the pixel-by-pixel adjustment loss (L_{pix}). Furthermore, when the overall adjustment loss (L_{over}) is removed, the accuracy decreases by 3.53%, from 94.85% to 91.32%. The temporal consistency loss (L_{tc}) is employed to constrain the Time-Consistency module better, thereby extracting more effective features in the temporal dimension, and when it is removed, the accuracy decreases by 2.82%, dropping from 94.85% to 92.03%. Finally, when combining all the loss functions with our method, the model achieves optimal performance on accuracy metrics, which demonstrates that our loss functions are reasonable. More ablation experiments are included in the Supplemental Materials.

Parameter Setting Analysis. As shown in Table 6, to determine the optimal parameter setting of μ_{out} , we examine how the average brightness of the normal-light image on ARID1.5, highlighting that $\mu_{out} = 0.5$ achieves the highest Top-1 accuracy.

μ_{out}	0.3	0.4	0.5	0.6	0.7
Top-1 (%)	90.32	92.23	94.85	94.23	92.76

Table 6. Accuracy of Different μ_{out} Configurations on ARID1.5.

	$h_i^x * X$	$h_i^x * Y$
Top-1 (%)	94.85	89.64

Table 7. Comparison of recognition performance using generated kernels with input X vs. Y .

LAM Analysis. The LAM module uses the generated convolution kernels h_i^x to convolve with the input X to obtain the enhanced image instead of directly using Y . This is because the Gamma transformation has inherent limitations. Its global monotonic mapping makes it difficult to handle multi-scale light distortion and preserve high-frequency details. Our experimental results in Table 7 show that fusing the generated kernels with the input’s spatiotemporal features significantly outperforms directly convolving

with Y in recognition performance.

4.4. Qualitative Results

Visual Analysis of Temporal Constraint Effectiveness.

We compare the RGB-Differences of our OwlSight with and without temporal constraint (TCM and L_{TC}). As Figure 5 shows, method in the upper part, which generates confused RGB-Differences (chaotic and unclear), fails to improve the action recognition performance in dark videos. Method in the bottom part indicates that our OwlSight, which generates clear RGB-Differences, succeeds in enhancing the action recognition performance in dark videos. The clean static background and clear motion boundaries demonstrates that the spatio-temporal consistency is well preserved by the introduced temporal constraint strategy. In summary, only the dark enhancement method, which can maintain the temporal consistency of dark videos, is beneficial to dark video action recognition. More analysis experiments are included in the Supplemental Materials.

5. Conclusion

We propose a novel biomimetic design-based framework OwlSight, for low-light action recognition by fully exploiting the brightness information. OwlSight comprises three key components: lightweight TCM, LAM, and RAM. The TCM captures the spatiotemporal relationships within dark videos. LAM dynamically adjusts the global brightness based on the input feature illumination. RAM enhances action recognition by maximizing the available illumination information. In addition, we construct a large-scale new dataset Dark-101, comprising 18,310 low-light video samples with 101 action categories. Extensive experiments demonstrate that our OwlSight achieves the outstanding performance for diverse datasets with a significant gain in accuracy compared to the prior methods.

References

- [1] Gedas Bertasius, Heng Wang, and Lorenzo Torresani. Is space-time attention all you need for video understanding. In *In Proc. International Conference on Machine Learning*, page 4, 2021. 7, 2
- [2] Yuanhao Cai, Hao Bian, Jing Lin, Haoqian Wang, Radu Timofte, and Yulun Zhang. Retinexformer: One-stage retinex-based transformer for low-light image enhancement. In *In Proc. IEEE International Conference on Computer Vision*, pages 12504–12513, 2023. 3
- [3] Joao Carreira and Andrew Zisserman. action recognition a new model and the kinetics dataset. In *In Proc. IEEE Conference on Computer Vision and Pattern Recognition*, pages 6299–6308, 2017. 3
- [4] Joao Carreira, Eric Noland, Chloe Hillier, and Andrew Zisserman. A short note on the kinetics-700 human action dataset. *arXiv preprint arXiv:1907.06987*, 2019. 6, 1
- [5] Chi-Jui Chang, Oscar Tai-Yuan Chen, and Vincent S Tseng. DI-kdd: Dual-light knowledge distillation for action recognition in the dark. *arXiv preprint arXiv:2406.02468*, 2024. 6, 7
- [6] Rui Chen, Jiajun Chen, Zixi Liang, Huaien Gao, and Shan Lin. Darklight networks for action recognition in the dark. In *In Proc. IEEE Conference on computer vision and pattern recognition*, pages 846–852, 2021. 3, 6, 7, 2
- [7] Christoph Feichtenhofer, Haoqi Fan, Jitendra Malik, and Kaiming He. Slowfast networks for video recognition. In *In Proc. IEEE International Conference on Computer Vision*, pages 6202–6211, 2019. 7, 2
- [8] Zhenqi Fu, Yan Yang, Xiaotong Tu, Yue Huang, Xinghao Ding, and Kai-Kuang Ma. Learning a simple low-light image enhancer from paired low-light instances. In *In Proc. IEEE Conference on computer vision and pattern recognition*, pages 22252–22261, 2023. 3
- [9] Huan Gao, Jichang Guo, Guoli Wang, and Qian Zhang. Cross-domain correlation distillation for unsupervised domain adaptation in nighttime semantic segmentation. In *2022 IEEE/CVF Conference on Computer Vision and Pattern Recognition (CVPR)*, pages 9903–9913, 2022. 2
- [10] P. Goyal, A. Ahuja, S. Kaur, and et al. Something-something v3: The road to better action recognition. In *In Proc. IEEE Conference on Computer Vision and Pattern Recognition*, pages 9588–9598, 2020. 6, 1
- [11] Chunle Guo, Chongyi Li, Jichang Guo, Chen Change Loy, Junhui Hou, Sam Kwong, and Runmin Cong. Zero-reference deep curve estimation for low-light image enhancement. In *In Proc. IEEE Conference on computer vision and pattern recognition*, pages 1780–1789, 2020. 2
- [12] Kensho Hara, Hirokatsu Kataoka, and Yutaka Satoh. Can spatiotemporal 3d cnns retrace the history of 2d cnns and imagenet. In *In Proc. IEEE conference on Computer Vision and Pattern Recognition*, pages 6546–6555, 2018. 2
- [13] Yifan Jiang, Xinyu Gong, Ding Liu, Yu Cheng, Chen Fang, Xiaohui Shen, Jianchao Yang, Pan Zhou, and Zhangyang Wang. Enlightengan: Deep light enhancement without paired supervision. *IEEE transactions on image processing*, 30:2340–2349, 2021. 3
- [14] Min Su Kim, Min Seok Kim, Mincheol Lee, Hyuk Jae Jang, Do Hyeon Kim, Sehui Chang, Minsung Kim, Hyojin Cho, Jiwon Kang, Changsoon Choi, Jung Pyo Hong, Do Kyung Hwang, Gil Ju Lee, Dae-Hyeong Kim, and Young Min Song. Feline eye-inspired artificial vision for enhanced camouflage breaking under diverse light conditions. *Science Advances*, 10(38):eadp2809, 2024. 2
- [15] Kunchang Li, Yali Wang, Yanan He, Yizhuo Li, Yi Wang, Limin Wang, and Yu Qiao. Uniformerv2: Spatiotemporal learning by arming image vits with video uniformer. *arXiv preprint arXiv:2211.09552*, 2022. 7, 2
- [16] Tianjiao Li, Jun Liu, Wei Zhang, Yun Ni, Wenqian Wang, and Zhiheng Li. Uav-human: A large benchmark for human behavior understanding with unmanned aerial vehicles. In *In Proc. IEEE Conference on computer vision and pattern recognition*, pages 16266–16275, 2021. 2, 4
- [17] Wenhao Li, Guangyang Wu, Wenyi Wang, Peiran Ren, and Xiaohong Liu. Fastllve: Real-time low-light video enhancement with intensity-aware look-up table. In *In Proc. ACM International Conference on Multimedia*, pages 8134–8144, 2023. 3
- [18] Yanghao Li, Chao-Yuan Wu, Haoqi Fan, Kartikeya Mangalam, Bo Xiong, Jitendra Malik, and Christoph Feichtenhofer. Mvitv2: Improved multiscale vision transformers for classification and detection. In *In Proc. IEEE Conference on computer vision and pattern recognition*, pages 4804–4814, 2022. 4, 7, 2
- [19] Seokjae Lim and Wonjun Kim. Dslr: Deep stacked laplacian restorer for low-light image enhancement. *IEEE Transactions on Multimedia*, 23:4272–4284, 2020. 3
- [20] Ji Lin, Chuang Gan, and Song Han. Tsm: Temporal shift module for efficient video understanding. In *In Proc. IEEE International Conference on Computer Vision*, pages 7083–7093, 2019. 7, 2
- [21] Ze Liu, Yutong Lin, Yue Cao, Han Hu, Yixuan Wei, Zheng Zhang, Stephen Lin, and Baining Guo. Swin transformer: Hierarchical vision transformer using shifted windows. In *In Proc. IEEE International Conference on Computer Vision*, pages 10012–10022, 2021. 2
- [22] Ze Liu, Jia Ning, Yue Cao, Yixuan Wei, Zheng Zhang, Stephen Lin, and Han Hu. Video swin transformer. In *In Proc. IEEE Conference on computer vision and pattern recognition*, pages 3202–3211, 2022. 7, 2
- [23] Kun Lu and Lihong Zhang. Tbefn: A two-branch exposure-fusion network for low-light image enhancement. *IEEE Transactions on Multimedia*, 23:4093–4105, 2020. 3
- [24] Feifan Lv, Feng Lu, Jianhua Wu, and Chongsoon Lim. Mbllen: Low-light image/video enhancement using cnns. In *In Proc. British Machine Vision Conference*, page 4, 2018. 3
- [25] M. Monfort, S. Jain, M. Kim, and et al. Moments in time dataset: One million videos for event understanding. In *In Proc. IEEE International Conference on Computer Vision*, pages 4020–4029, 2019. 6, 1
- [26] Zhaofan Qiu, Ting Yao, and Tao Mei. Learning spatiotemporal representation with pseudo-3d residual networks. In *In Proc. IEEE International Conference on Computer Vision*, pages 5533–5541, 2017. 3, 7

- [27] Hao Shao, Shengju Qian, and Yu Liu. Temporal interlacing network. In *In Proc. AAAI Conference on Artificial Intelligence*, pages 11966–11973, 2020. 2
- [28] Yiqi Shi, Duo Liu, Liguang Zhang, Ye Tian, Xuezhi Xia, and Xiaojing Fu. Zero-ig: Zero-shot illumination-guided joint denoising and adaptive enhancement for low-light images. In *In Proc. IEEE Conference on Computer Vision and Pattern Recognition*, pages 3015–3024, 2024. 5, 1
- [29] Himanshu Singh, Saurabh Suman, Badri Narayan Subudhi, Vinit Jakhethiya, and Ashish Ghosh. Action recognition in dark videos using spatio-temporal features and bidirectional encoder representations from transformers. *IEEE Transactions on Artificial Intelligence*, 4(6):1461–1471, 2022. 6, 7
- [30] Saurabh Suman, Nilay Naharas, Badri Narayan Subudhi, and Vinit Jakhethiya. Two-streams: dark and light networks with graph convolution for action recognition from dark videos (student abstract). In *In Proc. AAAI Conference on Artificial Intelligence*, pages 16340–16341, 2023. 3, 7
- [31] Du Tran, Lubomir Bourdev, Rob Fergus, Lorenzo Torresani, and Manohar Paluri. Learning spatiotemporal features with 3d convolutional networks. In *In Proc. IEEE International Conference on Computer Vision*, pages 4489–4497, 2015. 3
- [32] Du Tran, Heng Wang, Lorenzo Torresani, Jamie Ray, Yann LeCun, and Manohar Paluri. A closer look at spatiotemporal convolutions for action recognition. In *In Proc. IEEE Conference on Computer Vision and Pattern Recognition*, pages 6450–6459, 2018. 3, 7
- [33] Danai Triantafyllidou, Sean Moran, Steven McDonagh, Sarah Parisot, and Gregory Slabaugh. Low light video enhancement using synthetic data produced with an intermediate domain mapping. In *In Proc. European Conference on Computer Vision*, pages 103–119, 2020. 3
- [34] Zhigang Tu, Yuanzhong Liu, Yan Zhang, Qizi Mu, and Jun-song Yuan. Dtcn: Joint optimization of dark enhancement and action recognition in videos. *IEEE Transactions on Image Processing*, 32:3507–3520, 2023. 2, 4, 5, 6, 7, 1
- [35] A. Ulhaq. Action recognition in the dark via deep representation learning. In *IEEE International Conference on Image Processing, Applications and Systems (IPAS)*, pages 131–136, 2018. 3
- [36] Limin Wang, Yuanjun Xiong, Zhe Wang, Yu Qiao, Dahua Lin, Xiaoou Tang, and Luc Van Gool. Temporal segment networks: Towards good practices for deep action recognition. In *In Proc. European conference on computer vision*, pages 20–36. Springer, 2016. 7, 2
- [37] Li-Wen Wang, Zhi-Song Liu, Wan-Chi Siu, and Daniel PK Lun. Lightning network for low-light image enhancement. *IEEE Transactions on Image Processing*, 29:7984–7996, 2020. 3
- [38] Ruixing Wang, Qing Zhang, Chi-Wing Fu, Xiaoyong Shen, Wei-Shi Zheng, and Jiaya Jia. Underexposed photo enhancement using deep illumination estimation. In *In Proc. IEEE Conference on computer vision and pattern recognition*, pages 6849–6857, 2019. 3
- [39] Yuecong Xu, Jianfei Yang, Haozhi Cao, Kezhi Mao, Jianxiong Yin, and Simon See. Arid: A new dataset for recognizing action in the dark. In *Deep Learning for Human Activity Recognition: Second International Workshop, IJCAI-PRICAI*, pages 70–84, 2021. 1, 2, 4, 5, 6, 7
- [40] Qingsen Yan, Yixu Feng, Cheng Zhang, Pei Wang, Peng Wu, Wei Dong, Jinqiu Sun, and Yanning Zhang. You only need one color space: An efficient network for low-light image enhancement. *arXiv preprint arXiv:2402.05809*, 2024. 3
- [41] Yuwei Yin, Miao Liu, Renjie Yang, Yuanzhong Liu, and Zhigang Tu. Dark-dsar: Lightweight one-step pipeline for action recognition in dark videos. *Neural Networks*, 179:106622, 2024. 4, 6, 7, 2
- [42] Runsheng Yu, Wenyu Liu, Yasen Zhang, Zhi Qu, Deli Zhao, and Bo Zhang. Deepexposure: Learning to expose photos with asynchronously reinforced adversarial learning. In *Proc. Advances in neural information processing systems*, 31, 2018. 2
- [43] Anqi Zhu, Lin Zhang, Ying Shen, Yong Ma, Shengjie Zhao, and Yicong Zhou. Zero-shot restoration of underexposed images via robust retinex decomposition. In *In Proc. IEEE International Conference on Multimedia and Expo (ICME)*, pages 1–6, 2020. 2
- [44] Minfeng Zhu, Pingbo Pan, Wei Chen, and Yi Yang. Eemefn: Low-light image enhancement via edge-enhanced multi-exposure fusion network. In *In Proc. AAAI conference on artificial intelligence*, pages 13106–13113, 2020. 1, 3

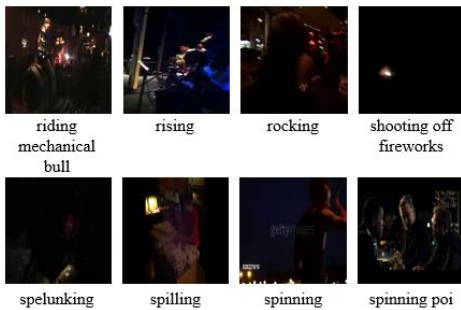


Figure 7. Example action classes from our Dark-101 datasets.

101 dataset are shown in Figure 7. And the visualization of the distribution of the number of datasets can be further viewed in the externally provided HTML file by clicking action items.

C. Quantitative Comparisons

C.1. Dark48

Evaluation on the Dark-48 [34] dataset. Dark-48 [34] provides a larger and more diverse collections than ARID and ARID1.5, featuring 48 action categories and 8,815 video clips, which enhances the range of testing conditions in low-light scenarios. Our proposed OwlSight achieves the highest accuracy 48.24%, surpasses the recent approaches by a margin of at least 1.56%.

Model	Top-1 (%)
TSN [36]	26.04
TSM [20]	36.46
TIN [27]	33.38
3D-ResNext-101 [12]	37.23
SlowFast16+64 [7]	39.58
TimeSformer-L [1]	43.27
Video-Swin-B [22]	41.92
MViT-B [18]	40.37
Dark-DSAR [41]	42.33
DarkLight-ResNext101 [6]	42.27
DTCM* [34]	46.68
OwlSight	48.24

Table 8. Comparison with state-of-the-arts on Dark-48 [34].

C.2. Dark101

Evaluation on our Dark-101 Dataset. These existing datasets are small-scale with insufficient number of categories, causing they are difficult to capture the diversity and complexity needed for training large-scale low-light action

recognition models. To promote real-world low-light action recognition research and test the generalization capacity of the proposed OwlSight, a comprehensive comparison is conducted on our new dataset *i.e.* Dark-101. As shown in Table 9, our OwlSight obtains an improvement of 1.72% over the other models, due to that it can fully exploit the illumination information and easily adapts to larger and more diverse dark action recognition datasets, meaning that it possesses stronger generalization capacity.

Model	Top-1 (%)
TimeSformer-L* [1]	36.39
Swin-B* [21]	37.79
Video-Swin-B* [22]	40.79
UniFormerV2* [15]	42.39
MViTv2-B* [18]	47.43
DTCM* [34]	50.91
Dark-DSAR* [41]	52.13
OwlSight	53.85

Table 9. Comparison with state-of-the-arts on our Dark-101.

D. RAM Analysis.

Since RAM performs exceptionally well, to demonstrate that the enhancement of the experimental results stems from the principle of the module we designed rather than the enlargement of the number of model parameters, we carried out an ablation experiment regarding the number of parameters of RAM. Specifically, when the RAM module is removed, the total number of parameters in the entire model is 51.4M. When the RAM module is incorporated, the total number of parameters in the entire model is 54.7M, where an increasing of merely 3.3M. However, the Top-1 accuracy increased by 3.03%. This experimental outcome verifies that the improvement in our experimental results is not attributed to the expansion of the parameter scale, as shown in Table 10.

	w/	w/o
Top-1 (%)	94.85	91.82
Params (M)	54.7	51.4

Table 10. Ablation study of RAM on the ARID1.5 dataset. The results show the impact of including and excluding the RAM module on the model’s performance and parameter count.

E. Visualize the attention.

As shown in Figure 8, we visualize the attention of our OwlSight and compare it with DTCM [34]. The selected actions, “Drink,” “Pick,” and “Stand” from the ARID1.5 dataset, are used for comparison. In the Grad-CAM map

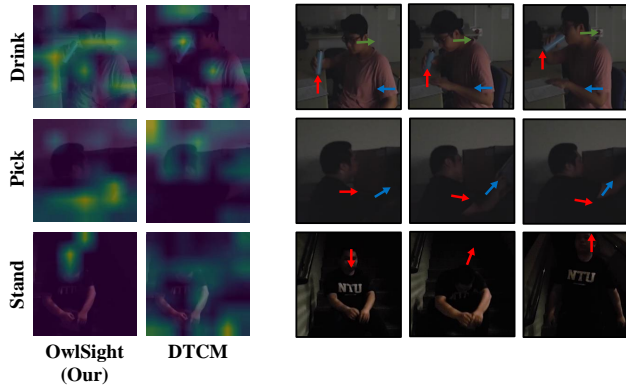


Figure 8. The left figure displays the Grad-CAM visualizations for three selected actions (“Drink”, “Pick” and “Stand”) from the ARID1.5 dataset. The gradients for the Grad-CAM maps are extracted from the second-to-last layer of our OwlSight and DTCM. The right side illustrates the full sequence of actions, with arrows indicating the movement trends of different body parts.

(left side of Figure 8), regions with action movements are highlighted. For the “Drink” action, it is clear that our OwlSight focuses on motion changes with higher illumination compared to DTCM. For the “Pick” action, our OwlSight provides a more accurate depiction of the motion changes, whereas DTCM tends to focus more on the general scene. For the “Stand” action, our OwlSight effectively captures the primary movement, while DTCM includes a significant amount of irrelevant background information.

On the right side of Figure 8, the entire action sequence is displayed, with arrows indicating the movement trends of different body parts. For example, the blue arrow in the “Pick” action highlights the arm movement, which is given significant attention. These results demonstrate that our model can accurately capture motion changes in low-light scenarios meanwhile reducing focus on irrelevant areas.